Electrophilic Addition vs Electron Transfer for the Interaction of Ag^+ with Molybdenum(II) Hydrides. 1. Reaction with $CpMoH(PMe_3)_3$ and the Mechanism of Decomposition of $[CpMoH(PMe_3)_3]^+$

James C. Fettinger,[†] Heinz-Bernard Kraatz,[†,¶] Rinaldo Poli,*[,‡] Elsje Alessandra Quadrelli,[†] and Raymund C. Torralba[†]

Department of Chemistry and Biochemistry, University of Maryland, College Park, Maryland 20742, and Laboratoire de Synthèse et d'Electrosynthèse Organometalliques, Faculté des Sciences "Gabriel", Université de Bourgogne, 6 Boulevard Gabriel, 21100 Dijon, France

Received July 8, 1998

The compound $CpMoH(PMe_3)_3$, **1**, is oxidized by Ag^+ in acetonitrile to the 17-electron complex $[CpMoH(PMe_3)_3]^+$, $[\mathbf{1}]^+$, which is indefinitely stable at low temperature. The oxidation takes place without the observation of a silver adduct intermediate. Complex $[\mathbf{1}]^+$ has also been generated by ferrocenium oxidation or by anodic oxidation and characterized by EPR spectroscopy. Complex $[\mathbf{1}]^+$ slowly decomposes at room temperature by a second-order rate law ($v = k_{disp}[\mathbf{1}^+]^2$), consistent with a disproportionation mechanism. In the presence of unoxidized **1**, on the other hand, the decomposition of $[\mathbf{1}]^+$ is faster and proceeds via a deprotonation mechanism ($v = k_{deprot}[\mathbf{1}^+][\mathbf{1}]$) with compound **1** acting as a catalyst. The ratio of the two second-order rate constants is $k_{deprot}/k_{disp} = 5.8(7)$). Intermediates of the disproportionation pathway, the solvent-stabilized double-oxidation products $[CpMoH(S)(PMe_3)_3]^{2+}$ (S = THF, MeCN), have been isolated as stable salts with the PF_6^- and BF_4^- counterions, respectively. The acetonitrile adduct has also been characterized by X-ray crystallography. The complex $[CpMoH(MeCN)(PMe_3)_3]^{2+}$ slowly transfers a proton to complex **1** to afford a 1:1 mixture of $[CpMo(PMe_3)_3(MeCN)]^+$ and $[CpMo(PMe_3)_3H_2]^+$ and is also slowly deprotonated by NEt_3.

Downloaded by CARLI CONSORTIUM on June 30, 2009
Published on November 21, 1998 on http://pubs.acs.org | doi: 10.1021/om9805786

Introduction

Transition metal hydrides pose an interesting question in terms of their reaction with electrophiles. The electrophilic reagent can attack the electron density at either the hydride ligand or the metal directly (when there are filled metal-based orbitals), in both cases affording electrophilic addition products. In addition, an electron-transfer process may occur (Scheme 1).

The protonation reaction, an extensively studied process, affords either classical $M(H)_2$ or nonclassical $M(H_2)$ dihydrides by pathways *a* and *b*, respectively (see Scheme 1).[1−13] The 3c-2e nonclassical product may be unstable and may collapse to the dihydrido complex or reductively eliminate dihydrogen (see Scheme 1, paths *b.i* and *b.ii*, respectively). The hydride abstraction reaction by the trityl cation ($E^+ = Ph_3C^+$)[14−17] can also be viewed as an example of a reaction following path *b.ii*.

Scheme 1

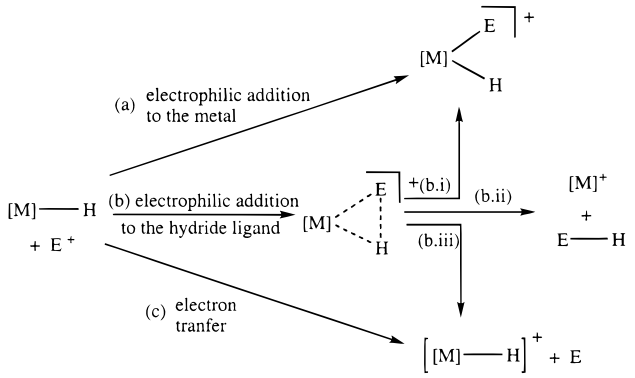

* Corresponding author. Tel: +33-(0)380396881. Fax: +33-(0)-380396098. E-mail: poli@u-bourgogne.fr.
† University of Maryland.
¶ Current address: Department of Chemistry, University of Saskatchewan, Saskatoon, SK S7N 5C9, Canada.
‡ Université de Bourgogne.

(1) Crabtree, R. H. *Acc. Chem. Res.* **1990**, *23*, 95−101.
(2) Parkin, G.; Bercaw, J. E. *J. Chem. Soc., Chem. Commun.* **1989**, 255−257.
(3) Lundquist, E. G.; Folting, K.; Streib, W. E.; Huffman, J. C.; Eisenstein, O.; Caulton, K. G. *J. Am. Chem. Soc.* **1990**, *112*, 855−863.
(4) Earl, K. A.; Jia, G.; Maltby, P. A.; Morris, R. H. *J. Am. Chem. Soc.* **1991**, *113*, 3027−3039.
(5) Arliguie, T.; Chaudret, B.; Jalon, F. A.; Otero, A.; Lopez, J. A.; Lahoz, F. J. *Organometallics* **1991**, *10*, 1888−1896.
(6) Heinekey, D. M. *Organometallics* **1991**, *10*, 2891−2895.
(7) Luo, X.-L.; Michos, D.; Crabtree, R. H. *Organometallics* **1992**, *11*, 237−241.
(8) Costello, M. T.; Fanwick, P. E.; Green, M. A.; Walton, R. A. *Inorg. Chem.* **1992**, *31*, 2359−2365.
(9) Bianchini, C.; Linn, K.; Masi, D.; Peruzzini, M.; Polo, A.; Vacca, A.; Zanobini, F. *Inorg. Chem.* **1993**, *32*, 2366−2376.
(10) Michos, D.; Luo, X.-L.; Faller, J. W.; Crabtree, R. H. *Inorg. Chem.* **1993**, *32*, 1370−1375.
(11) Jia, G.; Ng, W. S.; Yao, J.; Lau, C.-P.; Chen, Y. *Organometallics* **1996**, *15*, 5039−5045.
(12) Kim, Y.; Deng, H.; Gallucci, J. G.; Wojcicki, A. *Inorg. Chem.* **1996**, *35*, 7166−7173.
(13) Heinekey, D. M.; Radzewich, C. E.; Voges, M. H.; Schomber, B. M. *J. Am. Chem. Soc.* **1997**, *119*, 4172−4181.

10.1021/om9805786 CCC: $15.00 © 1998 American Chemical Society
Publication on Web 11/21/1998

Downloaded by CARLI CONSORTIUM on June 30, 2009
Published on November 21, 1998 on http://pubs.acs.org | doi: 10.1021/om9805786

Gold-based electrophiles, especially $AuPPh_3^+$, have also been extensively investigated.[18,19] These typically afford 3c-2e M(μ-H)Au moieties that can be seen as the isolobal analogues of the nonclassical dihydrides.[20] The substitution of H^+ for $AuPh_3^+$ typically affords more stable products. This has been the case for the particular complex $CpMoH(CO)_2(PMe_3)$, one of the rare mononuclear hydride complexes for which the comparative reactivity with *both* the proton and the $AuPPh_3^+$ reagent has been investigated.[21]

The silver ion has also been extensively investigated as an electrophilic reagent toward transition metal hydride complexes. The typical pathway is the attack at the M−H electron density, to afford complexes analogous to those obtained with the gold reagents (i.e., path *b* in Scheme 1).[22−33] However, silver also has oxidizing properties, and a possible alternative reaction pathway is electron transfer to afford metallic silver and the 17-electron hydride complex. This transformation can occur in principle with or without prior coordination of the silver ion to the nucleophilic M−H bond (paths *b.iii* and *c* in Scheme 1, corresponding to outer- and inner-sphere electron-transfer pathways, respectively). An example of an inner-sphere electron transfer via formation of a M(μ-H)Ag moiety has been shown recently.[34]

The $CpMoH(CO)_n(PMe_3)_{3-n}$ series of complexes have attracted our attention because there is a ca. 2 V difference between the oxidation potentials of the two extreme members of the series (n = 3 and 0), thus potentially influencing the reactivity of the Mo−H functionality toward the Ag^+ reagent. This paper presents the results of our investigations of the reactivity of complex $CpMoH(PMe_3)_3$, **1**, with the silver ion. The corresponding reactivity of the complex $CpMoH(CO)_2(PMe_3)$ and a comparison between the two systems are presented in part 2.[35] The studies reported here also provided new findings of relevance to the decomposition of 17-electron hydride complexes by the competitive deprotonation and disproportionation mechanisms.

Experimental Section

General Procedures. All operations were carried out under an atmosphere of dinitrogen with standard Schlenk-line techniques. Solvents were purified by conventional methods and distilled under argon prior to use (THF and Et_2O from Na/benzophenone, heptane from Na, acetone from $CaSO_4$, CH_2Cl_2 from P_4O_{10}, and MeCN form CaH_2). Deuterated solvents (C_6D_6, CD_3CN, THF-d_8, and CD_3COCD_3) were degassed by three freeze−pump−thaw cycles and then stored over 4 Å molecular sieves under dinitrogen. NMR spectra were obtained with Bruker WP200 and AF400 spectrometers. The peak positions are reported with positive shifts downfield of TMS as calculated from the residual solvent peaks (^{1}H) or downfield of external 85% H_3PO_4 (^{31}P). For each ^{31}P NMR spectrum, a sealed capillary containing H_3PO_4 was immersed in the same NMR solvent used for the measurement, and this was used as reference. EPR spectra were recorded on a Brucker ER200 spectrometer upgraded to ESP 300, equipped with a cylindrical ER/4103 TM 110 cavity and an X-band microwave generator. Cyclic voltammograms were recorded with an EG&G 362 potentiostat interfaced with MacLab hardware/software; the electrochemical cell was a locally modified Schlenk tube with a Pt counter electrode, a Pt working electrode, and a Ag/AgCl reference electrode. All potentials are reported vs the Cp_2Fe^+/Cp_2Fe couple, which was introduced in the cell at the end of each measurement. The EPR spectroelectrochemistry studies were performed with a home-built cell quite similar to one described in the literature,[36] the difference being that the aqueous reference electrode was replaced with a silver wire pseudoreference. Stopcocks and O-ring connections were added to allow all operations to be carried out under an inert atmosphere. Measurements were carried out on the Brucker ER200 spectrometer mentioned above, and the EPR species was generated from 0.1−0.2 M solutions by application of a constant current of 1 mA with an EG&EG 363 galvanostat. A control experiment of the nitrobenzene radical anion, generated at room temperature, yielded an EPR spectrum with greater resolution relative to that obtained with the analogous cell described in the literature.[36] Elemental (C, H, N) analyses were performed by MHW laboratories (Phoenix, AZ) and the analytical service at the LSEO at the Université de Bourgogne. Compound **1** was prepared as previously published.[37] Since this is very soluble in saturated hydrocarbons and cannot be easily crystallized, it was always prepared in situ in THF from equimolar amounts of $CpMoCl(PMe_3)_3$ and $LiBHEt_3$, followed by evaporation to dryness, extraction into *n*-heptane, filtration, and evaporation to dryness. In each case, the product purity was verified by ^{1}H NMR spectroscopy. $AgBF_4$, $FcPF_6$, and Cp_2Co were purchased from Aldrich and used as received.

(14) Sünkel, K.; Ernst, H.; Beck, W. *Z. Naturforsch.* **1981**, *36b*, 474−481.
(15) Smith, K.-T.; Tilset, M. *J. Organomet. Chem.* **1992**, *431*, 55−64.
(16) Ryan, O. B.; Tilset, M.; Parker, V. *D. J. Am. Chem. Soc.* **1990**, *112*, 2618−2626.
(17) Cheng, T.-Y.; Bullock, R. M. *Organometallics* **1995**, *14*, 4031−4033.
(18) Mueting, A. M.; Bos, W.; Alexander, B. D.; Boyle, P. D.; Casalnuovo, J. A.; Balaban, S.; Ito, L. N.; Johnson, S. M.; Pignolet, L. H. *New J. Chem.* **1988**, *12*, 505.
(19) Mingos, D. M. P.; Watson, M. J. In *Adv. Inorg. Chem.*; Sykes, A. G., Ed.; Academic Press: San Diego, 1992; Vol. 39; pp 327−399.
(20) Crabtree, R. H. *Angew. Chem., Int. Ed. Engl.* **1993**, *32*, 789−805.
(21) Galassi, R.; Poli, R.; Quadrelli, E. A.; Fettinger, J. C. *Inorg. Chem.* **1997**, *36*, 3001−3007.
(22) Green, M.; Orpen, A. G.; Salter, I. D.; Stone, F. G. A. *J. Chem. Soc., Chem. Commun.* **1982**, 813−814.
(23) Hutton, A. T.; Pringle, P. G.; Shaw, B. L. *Organometallics* **1983**, *2*, 1889−1891.
(24) Freeman, M. J.; Green, M.; Orpen, A. G.; Salter, I. D.; Stone, F. G. A. *J. Chem. Soc., Chem. Commun.* **1983**, 1332−1334.
(25) Connelly, N. G.; Howard, J. A. K.; Spencer, J. L.; Woodley, P. K. *J. Chem. Soc., Dalton Trans.* **1984**, 2003−2009.
(26) Rhodes, L. F.; Huffman, J. C.; Caulton, K. G. *J. Am. Chemn. Soc.* **1984**, *106*, 6874.
(27) Braunstein, P.; Gomes Carneiro, T. M.; Matt, D.; Tiripicchio, A.; Tiripicchio Camellini, M. *Angew. Chem., Int. Ed. Engl.* **1986**, *25*, 748−749.
(28) Alexander, B. D.; Johnson, B. J.; Johnson, S. M.; Boyle, P. D.; Kann, N. C.; Mueting, A. M.; Pignolet, L. H. *Inorg. Chem.* **1987**, *26*, 3506−3513.
(29) Albinati, A.; Lehner, H.; Venanzi, L. M.; Wolfer, M. *Inorg. Chem.* **1987**, *26*, 3933−3939.
(30) Albinati, A.; Demartin, F.; Venanzi, L. M.; Wolfer, M. K. *Angew. Chem., Int. Ed. Engl.* **1988**, *27*, 563−563.
(31) Albinati, A.; Anklin, C.; Janser, P.; Lehner, H.; Matt, D.; Pregosin, P. S.; Venanzi, L. M. *Inorg. Chem.* **1989**, *28*, 1105−1111.
(32) Albinati, A.; Chaloupka, S.; Demartin, F.; Koetzle, T. F.; Rüegger, H.; Venanzi, L. M.; Wolfer, M. K. *J. Am. Chem. Soc.* **1993**, *115*, 169−175.
(33) Antiñolo, A.; Carrillo, F.; Chaudret, B.; Fajardo, M.; García-Yuste, S.; Lahoz, F. J.; Lanfranchi, M.; López, J. A.; Otero, A.; Pellinghelli, M. A. *Organometallics* **1995**, *14*, 1297−1301.
(34) Rhodes, L. F.; Huffman, J. C.; Caulton, K. G. *Inorg. Chim. Acta* **1992**, *198−200*, 639−649.
(35) Quadrelli, E. A.; Poli, R. *Organometallics* **1998**, *17*, 5776.
(36) Allendoerfer, R. D.; Martinchek, G. A.; Bruckenstein, S. *Anal. Chem.* **1975**, *47*, 890.
(37) Abugideiri, F.; Kelland, M. A.; Poli, R.; Rheingold, A. L. *Organometallics* **1992**, *11*, 1303−1311.

Downloaded by CARLI CONSORTIUM on June 30, 2009
Published on November 21, 1998 on http://pubs.acs.org | doi: 10.1021/om9805786

Formation of $CpMoH(PMe_3)_3^+$, $[1]^+$. (a) Electrochemical Oxidation of 1 in THF. An aliquot of a THF solution (5 mL) of compound **1** (0.6 mmol) was introduced in the spectroelectrochemical cell containing Bu_4NPF_6 and the probe was cooled to −70 °C, followed by anodic oxidation at a constant current of 1 mA for 5 s. EPR: $g = 2.018$ (dq with Mo satellites, $a_d = 13.3$ G; $a_q = 29.3$ G; $a_{Mo} = 27$ G). The signal intensity remains constant at low temperature, whereas the line broadens and then slowly disappears upon warming to room temperature.

(b) Reaction of 1 with Ag^+ in THF. Solid $AgBF_4$ (68 mg; 0.35 mmol) was added to a THF solution of **1** (0.35 mmol) at −78 °C, resulting in the immediate formation of a dark brown precipitate. An aliquot of this reaction mixture was transferred and tested for EPR activity at −78 °C. The resulting EPR is identical to that obtained in the spectrochemical cell (see previous section) and assigned to $[\mathbf{1}]^+$. Upon warming to room temperature, the signal broadens and slowly disappears. A number of diamagnetic products appeared in the NMR spectrum after the solution was allowed to warm to room temperature. The nature of these decomposition products was not further investigated.

(c) Reaction of 1 with Cp_2Fe^+ in THF. Preparation of $[CpMoH(PMe_3)_3(THF)](PF_6)_2$, 2. A blue suspension of Cp_2FePF_6 (52 mg, 0.16 mmol) was prepared in THF (3 mL) and cooled to −80 °C in a cryostat. A yellow THF solution (5 mL) of 1 (0.17 mmol) was cooled to −80 °C and added dropwise to the ferrocenium suspension. The green mixture slowly bleached the blue color of the ferrocenium and induced the precipitation of a clear solid. After the suspension was let stir overnight in the cryostat, the light orange supernatant was filtered off. An aliquot showed weak EPR activity in the form of overlapping unassigned multiplets. Compound **2** was recovered through filtration as a light pink solid, washed with Et_2O (3 × 3 mL), and dried under vacuum (27 mg, 45% yield relative to ferrocenium). *Anal.* Calcd for $C_{18}H_{41}F_{12}MoOP_5$: C, 28.74; H, 5.49. Found: C, 28.07; H, 5.19. The solid is only slightly soluble in THF and acetonitrile and is not soluble in benzene and toluene.

Reduction of 2 to 1. The solid obtained by the procedure described in the previous section (15 mg; 20 μmol) was added to a solution of Cp_2Co (ca. 10 mg; 50 μmol) in C_6D_6 (0.4 mL), inducing the solubilization of the solid. The resulting solution was EPR silent and showed the resonances of THF and compound **1** in the correct relative intensities for a 1:1 molar ratio in the ^1H NMR spectrum.

EPR Monitoring of the Decomposition of $[1]^+$ in THF. An 80 μmol sample of **1** was suspended in THF (4 mL). $FcPF_6$ (26 mg, 79 μmol) was added to the solution, and immediate bleaching of the oxidant ensued. An aliquot of the orange solution was transferred to an EPR tube, and EPR spectra were recorded over time. The relative concentration of $[\mathbf{1}]^+$ was monitored by double integration of each spectrum (see Results).

EPR Monitoring of the Decomposition of $[1]^+$ in the Presence of 1 in THF. A 162 μmol sample of **1** was suspended in THF (4 mL). $FcPF_6$ (24 mg; 72 μmol) was added to the solution, and immediate bleaching of the oxidant ensued. An aliquot of the orange solution was transferred in an EPR tube, and EPR spectra were recorded over time and double-integrated (see Results).

Attempt at the EPR Monitoring of the Decomposition of $[1]^+$ in MeCN. Compound **1** (0.12 mmol) was dissolved in MeCN (5mL). $FcPF_6$ (39 mg; 0.12 mmol) was added, and discoloration of the oxidant blue color ensued. An aliquot of the solution was transferred in an EPR tube. The first EPR spectrum, taken 7 min after the addition of the oxidant, did not show any activity. The short lifetime of $[\mathbf{1}]^+$ in MeCN prevented the kinetic analysis of its decomposition by EPR.

Reaction of 1 with 1 equiv of Fc^+ in MeCN: Formation of $[CpMo(PMe_3)_3(MeCN)]^+$ and $[CpMo(PMe_3)_3(H)_2]^+$. A stock solution of **1** was prepared in CD_3CN (3 mL; 0.131 M), and its concentration was checked through integration against an interal standard of ferrocene. A 605 μL aliquot (79 μmol) was added to $FcPF_6$ (26 mg; 79 μmol). Immediate dissolution of the oxidant ensued to give an orange solution. The first acceptable NMR spectrum was obtained after 10 min from the addition. Earlier spectra were affected by poor shimming due to the presence of paramagnetic species in solution. The solution contained, in addition to ferrocene (^1H NMR resonance at δ 4.14), a 1:1 mixture of two molybdenum species: $[CpMo(PMe_3)_3(MeCN)]^+$ [^1H NMR (δ): 4.79 (s, 5H, Cp), 1.5 (vb, PMe_3). ^{31}P NMR (δ): 1 (vb, $w_{1/2} = 100$ Hz, 1P), −1 (vb, $w_{1/2} = 160$ Hz, 2P)] and $[CpMo(PMe_3)_3(H)_2]^+$ [^1H NMR (δ): 4.81 (m, $J = 1.2$ Hz, 5H, Cp), 1.47 (d, $J_P = 8.4$ Hz, 27H, PMe_3), −4.0 (vb, 1H, Mo−H). ^{31}P NMR (δ): 8 (vb, $w_{1/2} = 200$ Hz)]. Both complexes were independently synthesized (vide infra).

Reaction of 1 with 2 equiv of Fc^+ in MeCN: Formation of $[CpMo(PMe_3)_3(CD_3CN)H]^{2+}$. $FcPF_6$ (52 mg; 157 μmol) was introduced in a NMR tube. A 602 μL aliquot of the CD_3CN stock solution of **1** (see previous section, 79 μmol) was added. A complete discoloration ensued. After 20 min, the NMR spectra revealed the nearly exclusive formation of $[CpMoH(PMe_3)_3(CD_3CN)]^{2+}$ and ferrocene. ^1H NMR of $[CpMoH(PMe_3)_3(CD_3CN)]^{2+}$ (δ): 5.31 (m, $J = 1$ Hz, 5H, Cp), 1.61 (d, $J_P = 9$Hz, 18H, PMe_3), 1.57 (d, $J_P = 9$Hz, 9H, PMe_3). $^{31}P\{^1H\}$ NMR (CD_3CN, δ): 3.6 (t, $J = 26$ Hz, 1P); 0.5 (*d*, $J = 26$ Hz, 2P). $^{31}P\{$selec-$^1H\}$ NMR (CD_3CN, δ): 3.6 (td, $J_P = 26$ Hz, $J_H = 10$ Hz, 1P); 0.5 (dd, $J_P = 26$ Hz, $J_H = 10$ Hz, 2P).

Reaction of 1 with 1 equiv of Ag^+ in MeCN: Synthesis of $[CpMo(PMe_3)_3(MeCN)H]^{2+}(BF_4^-)_2$, 3. Compound **1** (0.12 mmol) and $AgBF_4$ (24 mg, 0.12 mmol) were mixed in CD_3CN (1.2 mL). The immediate reaction produced a black solid. The NMR investigation of the orange supematant showed the formation of $[CpMo(PMe_3)_3(CD_3CN)H]^{2+}$ as the major product. The black precipitate was removed from the mother solution through filtration, and diethyl ether was then added to the solution. Precipitation of an orange solid ensued, which was recovered by filtration and vacuum drying. The solid was washed with dichloromethane (2 × 2 mL), the red filtrates were removed, and the yellow microcrystalline solid was dried under vacuum (24 mg, 38% yield as **3**·Et_2O). An aliquot of the solid exhibited the resonances of $[CpMoH(PMe_3)_3(CD_3CN)]^{2+}$ and Et_2O in relative intensities as expected for a 1:1 molar ratio. Anal. Calcd for $C_{20}H_{43}D_3B_2F_8NMoOP_3$: C, 35.2; H, 6.35; D, 0.88; N, 2.05. Found: C, 35.6; H, 6.92; N, 1.57. Crystals of **3**·MeCN suitable for an X-ray crystallographic study were obtained from acetonitrile/ether solutions stored at −20 °C for 2 days.

Reaction of 1 with 2 equiv of Ag^+ in CD_3CN. Addition of $AgBF_4$ (35 mg, 181 μmol) to a solution of **1** (90 μmol) in CD_3CN (0.5 mL) generated $[CpMoH(PMe_3)_3(CD_3CN)]^{2+}$ as the main product. The ^1H NMR spectra were monitored over time (>2 days). No transformation to $[CpMo(PMe_3)_3(CD_3CN)]^+$ and $[CpMoH_2(PMe_3)_3]^+$ was observed.

Reaction of 3 with NEt_3. Crystals of compound **3** (ca. 2.0 mg, 3.1×10^{-3} mmol) were dissolved in CD_3CN (0.45 mL), and their purity was checked through ^1H NMR. NEt_3 (2.0 μL, 3.2×10^{-2} mmol) was added to the yellow solution. The resonances of $[CpMoH(PMe_3)_3(CD_3CN)]^{2+}$ slowly disappeared ($t_{1/2} = 2$ h), while those of $[CpMo(PMe_3)_3(CD_3CN)]^+$ increased. ^1H NMR (δ): 4.79 (s, 5H, Cp), 1.5 (vb, PMe_3). ^{31}P NMR (δ): 1 (vb, $w_{1/2} = 100$ Hz, 1P), −1 (vb, $w_{1/2} = 160$ Hz, 2P). No resonances attributable to other secondary products were detected by NMR.

Reaction of 3 with 1. A yellow solution of **1** (50 μmol) in CD_3CN (0.8 mL) was split in two halves. To one of them $AgBF_4$ (10 mg; 51 μmol) was added, forming $[CpMoH(PMe_3)_3(CD_3CN)]^{2+}$ and Ag. Afer the precipitate settled, the orange supernatant was added to the yellow original solution and the reaction was monitored through ^1H NMR. The

Table 1. Crystal Data and Structure Refinement for Compound 3·MeCN

empirical formula	$C_{18}H_{39}B_2F_8MoN_2P_3$
fw	645.98
temp	153(2) K
wavelength	0.71073 Å
cryst syst	orthorhombic
space group	*Pnma*
unit cell dimens	$a = 24.263(2)$ Å $\alpha = 90°$ $b = 14.663(2)$ Å $\beta = 90°$ $c = 7.9793(13)$ Å $\gamma = 90°$
volume, *Z*	2838.8(6) Å^3, 4
density (calcd)	1.511 Mg/m^3
abs coeff	0.694 mm^{-1}
F(000)	1320
θ range for data collection	2.18−25.04°
limiting indices	$-28 \le h < 28$, $-17 \le k < 17$, $-9 \le l < 9$
no. of reflns collected, independent	10283, 2624 [*R*(int) = 0.0997]
max. and min. transmission	0.8282 and 0.7430
refinement method	full-matrix least-squares on F^2
no. of data, restraints, params	2617, 41, 269
goodness-of-fit on F^2	1.111
final *R* indices [$I > 2\sigma(I)$]	R1 = 0.0391, wR2 = 0.0692 [1889 data]
R indices (all data)	R1 = 0.0729, wR2 = 0.0809
largest diff peak and hole	0.462 and −0.596 e Å^{-3}

Downloaded by CARLI CONSORTIUM on June 30, 2009
Published on November 21, 1998 on http://pubs.acs.org | doi: 10.1021/om9805786

formation of $[CpMo(PMe_3)_3(CD_3CN)]^+$ and $[CpMoH_2(PMe_3)_3]^+$ was discernible within the first minutes of the addition, but it was not complete until after more than 24 h.

Protonation of Compound 1. (a) In toluene. Synthesis of *mer*-$[CpMoH_2(PMe_3)_3]^+$ $[BF_4]^-$, 4. This procedure is a modification of that previously reported.[38] To a solution of **1** (0.367 mmol) in toluene (10 mL) cooled to −60 °C was added HBF_4 (54% in diethyl ether) (51 μL, 0.367 mmol) via microsyringe, causing the formation of an off-white precipitate. Stirring was continued for 10 min. Addition of heptane (5 mL) caused the precipitation of the product, which was filtered, washed with heptane (3 × 5 mL), and dried under vacuum to yield 134 mg (76%) of $[CpMoH_2(PMe_3)_3][BF_4]$. The ^{1}H NMR at room temperature corresponds to that previously reported.[38] Decoalescence of the hydride resonances is observed upon cooling to 238 K. ^{1}H NMR (δ, CD_3CN, 238 K): 4.81 (s, 5H, Cp), 1.46 (d, $J_{HP} = 8.4$ Hz, 27H, PMe_3), −2.48 (virtual qd, $J_{HP} = 52.5$ Hz, $J_{HH} = 8.4$ Hz, 1H, Mo−H_{eq}), −5.65 (virtual tt, $J_{HP} = 46.4$ Hz, $J_{HH} = 8.4$ Hz, 1H, Mo−H_{ax}). ^{31}P NMR: (δ, CD_3CN, 233 K): 10 (b, $w_{1/2} = 50$ Hz, 2P), 4 (b, $w_{1/2} = 50$ Hz, 1P). Selective decoupling experiments (^{1}H{selec-^{1}H} and ^{1}H{selec-^{31}P}) allowed all the individual coupling constants to be determined. A simulation of the experimental spectrum proved satisfactory. Complex **4** is stable in acetonitrile: no H_2 loss was observed over several months at room temperature or for 18 h at 80 °C.

(b) In MeCN. To a solution of **1** (75 μmol) in CD_3CN was added HBF_4 (54% in diethyl ether) (10 μL,72 mmol). Quantitative formation of **4** ensued. No transformation to $[CpMo(PMe_3)_3(CD_3CN)]^+$ was observed over several days.

(b) In Wet MeCN. To a solution of **1** (80 μmol) in CD_3CN (0.60 mL) was added H_2O (2 μmol, 0.1 mmol). The ^{1}H NMR resonances of **1** were not affected. Addition of HBF_4 (54% in diethyl ether) (10 μL,72 mmol) resulted in its transformation to **4** and did not shift the water peak resonance.

X-ray Crystallography for Compound 3·MeCN. A yellow needle with approximate dimensions 0.50 × 0.10 × 0.10 mm was placed on the Enraf-Nonius CAD-4 diffractometer. The cell parameters and crystal orientation matrix were determined from 25 reflections in the range $10.0 < \theta < 16.2°$ and further confirmed with axial photographs. Crystal parameters and selected collection and refinement parameters are collected in Table 1. Intensity standards showed no significant variation with time, and no decay correction was applied. The data were corrected for Lorentz and polarization factors and for absorption on the basis of the ψ-scan method.[39] Systematic absences indicated the centrosymmetric space group *Pnma* (no. 62) or the non-centrosymmetric space group $Pna2_1$ (no. 33), intensity statistics clearly favoring the centric case. The structure was determined by direct methods in SHELXTL, with the successful location of the four heavy atoms (Mo, 3P) and several carbon and nitrogen atoms. The remaining non-hydrogen atoms were found from several additional difference-Fourier maps. The Cp ring was found to be disordered, and its refinement yielded two partial occupancy fragments with relative occupancies of 0.57:0.43. One BF_4 molecule was found to be fully occupied, while the second one and the interstitial acetonitrile molecule were disordered in symmetry-related positions. Hydrogen atoms were allowed to ride on the parent carbon atom [d(C−H) = 0.950 Å; $U_H = 1.2U_{(parent)}$ for the Cp H atoms; d(C−H) = 0.980 Å, $U_H = 1.5U_{(parent)}$ for the Me H atoms, initially determined with a rotational difference-Fourier map about the central carbon atom]. The hydride was located directly from a difference-Fourier map and its parameters (*xyzU*) were all allowed to refine freely. During the final stages of the full-matrix least-squares refinement, all of the non-H atoms were refined anisotropically. Several restraints were applied to force the thermal parameters of the two sets of atoms comprising the Cp ring to remain positive definite. The function minimized was $\sum w(F_o^2 - F_c^2)$, where $w = 1/[\sigma^2(F_o^2) + (0.0331/P)^2 + 1.6302P]$ and $P = (\max(F_o^2,0) + 2F_c^2)/3$. An empirical correction for extinction was also attempted but found to produce a negative value and was not applied. Selected bond distances and angles are collected in Table 2.

Results and Discussion

(a) Electrochemical Oxidation of $CpMoH(PMe_3)_3$. Compound **1** undergoes a reversible oxidation process at $E_{1/2} = -1.46$ V vs the ferrocene standard in MeCN, contrary to the corresponding irreversible oxidation processes of complexes $CpMoH(CO)_3$ and $CpMoH(CO)_2L$ (L = PMe_3, PPh_3).[16,40] As expected, the oxidation potential of **1** is shifted negatively with respect to the potentials required to oxidize $CpMoH(CO)_2(PMe_3)$ ($E_{p,a}$

(38) Brookhart, M.; Cox, K.; Cloke, F. G. N.; Green, J. C.; Green, M. L. H.; Hare, P. M.; Bashkin, J.; Derome, A. E.; Grebenik, P. D. *J. Chem. Soc., Dalton Trans.* **1985**, 423−433.

(39) North, A. C. T.; Phillips, D. C.; Mathews, F. S. *Acta Crystallogr., Sect. A* **1968**, *A24*, 351−359.

(40) Quadrelli, E. A.; Kraatz, H.-B.; Poli, R. *Inorg. Chem.* **1996**, *35*, 5154−5162.

Table 2. Selected Bond Distances (Å) and Angles (deg) for Compound 3·MeCN

Mo(1)−CNT	1.980(11)	Mo(1)−P(2)	2.5108(11)
Mo(1)−CNT2	1.966(13)	Mo(1)−N(7)	2.144(5)
Mo(1)−P(1)	2.476(2)	Mo(1)−H(1A)	1.61(6)
P(1)−Mo(1)−P(2)	90.28(3)	CNT−Mo(1)−P(2)	110.27(9)
P(1)−Mo(1)−N(7)	143.36(13)	CNT−Mo(1)−N(7)	110.1(8)
P(1)−Mo(1)−H(1A)	66(2)	CNT−Mo(1)−H(1A)	173(2)
P(2)−Mo(1)−N(7)	77.26(5)	CNT2−Mo(1)−P(1)	106.9(8)
P(2)−Mo(1)−H(1A)	70.7(3)	CNT2−Mo(1)−P(2)	110.23(10)
N(7)−Mo(1)−H(1A)	77(2)	CNT2−Mo(1)−N(7)	109.7(8)
CNT−Mo(1)−P(1)	106.6(8)	CNT2−Mo(1)−H(1A)	173(2)

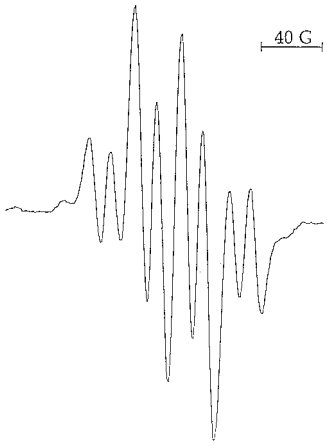

Figure 1. EPR spectrum of the $[CpMoH(PMe_3)_3]^+$ species in THF (T = 193 K).

= +0.26 V)[40] and $CpMoH(CO)_3$ ($E_{p,a}$ = +0.80 V).[16] This corresponds to a shift of ca. −0.54 V from the tricarbonyl to the dicarbonyl derivative, and to an average of ca. −0.86 V per CO/PMe_3 substitution from the dicarbonyl to the tris(phosphine) derivative. A shift of −0.56 V was correspondingly observed on going from $CpWH(CO)_3$ to $CpWH(CO)_2(PMe_3)$.[16] Similar trends upon CO/PR_3 substitution have been observed before for other systems, for instance CpRuHLL′ (L, L′ = CO, tertiary phosphine)[41−44] and Cp* analogues[45] and a variety of octahedral, d^6 dinitrogen, and η^2-dihydrogen complexes.[46]

The identity of the oxidation product of **1** as the corresponding 17-electron cation $[\mathbf{1}]^+$ has been verified by EPR spectroscopy. Constant-current bulk oxidation in THF at −70 °C in an EPR spectroelectrochemical cell rapidly afforded the EPR spectrum shown in Figure 1. The spectrum consists of a main doublet of quartets at g = 2.014 because of coupling to the hydride nucleus (a_H = 12.9 G) and the three phosphorus nuclei (a_P = 28.6 G). The main signal is flanked by satellites due to coupling to the I = 5/2 ^{95}Mo and ^{97}Mo nuclei (a_{Mo} = 27 G) in the corresponding isotopomers (total abundance ca. 25%). Half-sandwich, 17-electron Mo(III) derivatives are well-known to adopt a "four-legged piano stool" geometry (see for instance the X-ray structures of $[CpMoCl(PMe_3)_3]^+$).[37,47] If this is also the geometry adopted by $[\mathbf{1}]^+$, the phosphine ligands should give rise to a doublet of triplets rather than a quartet. However, hydride ligands are often highly mobile in the coordination sphere of transition metal complexes and isomerization processes are generally even faster in radical species;[48] therefore the three phosphine ligands may be rendered equivalent on the EPR time scale by a rapid fluxional process. Alternatives accounting for the equivalence of the phosphorus couplings are an accidental degeneracy of the two hyperfine splittings or a static structure with equivalent phosphine ligands, namely, a pseudo-tbp structure with Cp and H in the axial positions. However, all related tris(phosphine) Mo(III) complexes have significantly different phosphorus hyperfine splittings (for $[CpMoCl(PMe_3)_3]^+$ $a_{P(d)}$ = 26.0 G, $a_{P(t)}$ = 19.5 G;[37] for $[CpMoCl(triphos)]^+$ $a_{P(d)}$ = 28.0 G, $a_{P(t)}$ = 14.5 G[49]), and a pseudo-tbp structure has never been observed for this class of half-sandwich Mo(III) complexes.[50] Therefore, we consider it more likely that fluxionality is the reason for the EPR equivalence of the three phosphorus nuclei. The EPR spectrum of $[\mathbf{1}]^+$ becomes broader upon warming, and only a broad line with no distinguishable hyperfine splittings is observed at room temperature. The compound slowly decomposes at room temperature in THF, as indicated by the decrease of EPR intensity ($t_{1/2} \approx$ 30 min), while it appears to be indefinitely stable at −70 °C.

(b) Chemical Oxidation of $CpMoH(PMe_3)_3$ and Characterization of Its Kinetic and Thermodynamic Products. The 1:1 interaction of **1** with either Ag^+ or Cp_2Fe^+ in THF results in electron transfer, with formation of elemental silver or ferrocene, respectively, and the unstable radical complex $[\mathbf{1}]^+$; see eq 1, as shown by EPR spectroscopy. The interaction is instantaneous, without the formation of an observable hydride-bridged silver adduct.

$$\underset{\mathbf{1}}{CpMoH(PMe_3)_3} + X^+ \rightarrow X + \underset{[\mathbf{1}]^+}{[CpMoH(PMe_3)_3]^+} \quad (1)$$

$$(X = Ag,\ Cp_2Fe)$$

When reaction 1 is run in MeCN, the formation of $[\mathbf{1}]^+$ is not observed by EPR, presumably because of its fast decomposition in this solvent. The final products of the reaction are Ag or ferrocene, and a 1:1 mixture of

(41) Ryan, O. B.; Tilset, M.; Parker, V. D. *Organometallics* **1991**, *10*, 298−304.
(42) Ryan, O. B.; Tilset, M. *J. Am. Chem. Soc.* **1991**, *113*, 9554−9561.
(43) Ryan, O. B.; Smith, K.-T.; Tilset, M. *J. Organomet. Chem.* **1991**, *421*, 315−322.
(44) Smith, K.-T.; Rømming, C.; Tilset, M. *J. Am. Chem. Soc.* **1993**, *115*, 8681−8689.
(45) Jia, G.; Lough, A. J.; Morris, R. H. *Organometallics* **1992**, *11*, 161−171.
(46) Morris, R. H. *Inorg. Chem.* **1992**, *31*, 1471−1478.
(47) Fettinger, J. C.; Kraatz, H.-B.; Poli, R.; Rheingold, A. L. *Acta Crystallogr., Sect. C.* **1995**, *C51*, 364−367.
(48) *Organometallic Radical Processes*; Trogler, W. C., Ed.; Elsevier: Amsterdam, 1990; Vol. 22.
(49) Cole, A. A.; Mattamana, S. P.; Poli, R. *Polyhedron* **1996**, *15*, 2351−2361.
(50) Poli, R. *J. Coord. Chem. B* **1993**, *29*, 121−173.
(51) Volz, H.; Lotsch, W. *Tetrahedron Lett.* **1969**, *27*, 2275−2278.

Downloaded by CARLI CONSORTIUM on June 30, 2009
Published on November 21, 1998 on http://pubs.acs.org | doi: 10.1021/om9805786

complexes $[CpMo(PMe_3)_3(MeCN)]^+$ and $[CpMo(PMe_3)_3H_2]^+$; see eq 2.

$$2\underset{\mathbf{1}}{CpMoH(PMe_3)_3} + 2X^+ + MeCN \rightarrow [CpMo(PMe_3)_3(MeCN)]^+ + [CpMo(PMe_3)_3H_2]^+ + 2X \quad (2)$$

(X = Ag, Cp_2Fe)

Complex $[CpMo(PMe_3)_3H_2]^+$ has been previously reported from the protonation reaction of $CpMoH(PMe_3)_3$ and has been further investigated by us (see section e). Complex $[CpMo(PMe_3)_3(MeCN)]^+$, on the other hand, has not been previously described. It shows the two expected ^{31}P resonances in a 1:2 ratio and the correct integration for the Cp and PMe_3 resonances in the ^1H NMR spectrum. The ^1H NMR resonance of the MeCN ligand could not be observed, most likely because of a rapid exchange with the CD_3CN solvent. In an effort to independently synthesize this complex, we attempted to abstract the hydride ligand from **1** with the trityl cation. A similar reaction on the related $CpMoH(CO)_2(PR_3)$ (R = Me, Ph) cleanly afforded the expected $[CpMo(CO)_2(PR_3)(MeCN)]^+$.[15,40] Conversely, this reaction yields a mixture of $[CpMo(PMe_3)_3H_2]^+$, $[CpMo(MeCN)(PMe_3)_3]^+$, and $[CpMo(PMe_3)_3H(MeCN)]^{2+}$, even when carried out at lower than ambient temperatures. This result is consistent with the known reduction potentials of the trityl cation (+ 0.08 V vs Fc/Fc^+ [51]) and **1** (−1.46 V vs Fc/Fc^+, vide supra). This electron-transfer reaction also leads to a number of unidentified byproducts, which may result from side reactions such as attack of the trityl radical at the cyclopentadienyl ligand.[43] The other expected end product is the trityl radical, in equilibrium with its head-to-tail dimer, the latter being observed in the ^1H NMR spectrum. A spectroscopically pure solution of $[CpMo(PMe_3)_3(MeCN)]^+$ was eventually obtained by deprotonation of isolated $[CpMo(PMe_3)_3H(MeCN)]^{2+}$ (vide infra).

The formation of the products of reaction 2 is in agreement with the general reactivity observed for a series of closely related systems.[16,44] It is worth noticing that the solvent adduct is the only product of the oxidation of the very similar $CpMoH(CO)_2(PMe_3)$, the reaction otherwise proceeding with the same stoichiometry (1 equiv of oxidizing agent per Mo center) under anhydrous conditions.[40] This is so because the hypothetical product of proton transfer, $[CpMoH_2(CO)_2(PMe_3)]^+$, is unstable toward loss of H_2. The substitution of the two carbonyl ligands with as many phosphine ligands renders the dihydride product sufficiently electron-rich to prevent the expulsion of molecular hydrogen.

When the oxidation is carried out in the presence of *2* equiv of oxidant (either Fc^+ or Ag^+) in either THF or MeCN, dicationic hydride complexes $[CpMoH(PMe_3)_3(S)]^{2+}$ (S = THF, MeCN) are obtained (see eq 3). These complexes have been isolated as PF_6^- salt for S = THF (compound **2**) and as BF_4^- salt for S = MeCN (compound **3**). The complex $[CpMoH(PMe_3)_3(MeCN)]^{2+}$ has also been observed as a kinetic product during the oxidation with only 1 equiv of oxidant. When the reaction mixture was set for crystallization in the early stages of the oxidation, compound **3** was recovered as a the major product in a 38% yield.

$$\underset{\mathbf{1}}{CpMoH(PMe_3)_3} + 2X^+ + S \rightarrow 2X + [CpMoH(PMe_3)_3(S)]^{2+} \quad (3)$$

(X = Ag, Cp_2Fe; S = THF, MeCN)

Compound **2** is rather unstable in solution, preventing a spectroscopic characterization and leading to an analytically impure solid. Its isolation is permitted by its sparing solubility under the synthetic conditions. However, recovery of the precursor complex **1** by cobaltocene reduction of isolated **2** comes in strong support of our proposed formulation. The scant solubility of the dication and the variety of decomposition products have discouraged us to investigate this decomposition process in more detail. One of the various final products of decomposition has been recognized as the oxo complex $[CpMoO(PMe_3)_2]^+$, indicating that adventitious water favorably competes with THF for coordination to the Mo(IV) center of the dicationic hydrido complex. The role of water *as a ligand* during the oxidation of compound **1** under a variety of conditions will be the subject of a separate contribution.[52] A THF adduct deriving from the oxidation of $CpRe(PPh_3)_2H_2$ in THF, $[CpRe(PPh_3)_2(THF)H]^+$, has been described.[53]

Compound **3** is much more stable than compound **2** and could be recrystallized from $MeCN/Et_2O$, yielding analytically pure crystals that were investigated by NMR and X-ray crystallography. The inequivalent phosphine ligands give rise to two resonances in a 2:1 ratio in both the ^1H and the ^{31}P NMR spectrum, in agreement with the crystallographically determined structure (vide infra). While no resonance was observable in the ^1H NMR for the hydridic proton, its presence was confirmed by selective decoupling ^{31}P NMR experiments. The hydride resonance could not be hidden under the Cp* or PMe_3 resonances, because the latter ones were saturated in the selective decoupling experiment which reveals the P−hydride coupling. The coupling constants between the hydride and the two inequivalent sets of phosphorus nuclei are the same and relatively small (10 Hz), consistent with the observed *cis* arrangement. The geometry of the dication in the structurally characterized **3**·MeCN (see Figure 2) may be described as a pseudooctahedron when considering the Cp ligand as occupying a single coordination position. This geometry is analogous to that established for a number of other Cp-containing 18-electron complexes of Mo(IV) and W(IV).[54−61] As may be expected from

Downloaded by CARLI CONSORTIUM on June 30, 2009
Published on November 21, 1998 on http://pubs.acs.org | doi: 10.1021/om9805786

(52) Fettinger, J. C.; Kraatz, H.-B.; Poli, R.; Quadrelli, E. A. Submitted.
(53) Detty, M. R.; Jones, W. D. *J. Am. Chem. Soc.* **1987**, *109*, 5666−5673.
(54) Stärker, K.; Curtis, M. D. *Inorg. Chem.* **1985**, *24*, 3006−3010.
(55) Owens, B. E.; Poli, R. *Inorg. Chim. Acta* **1991**, *179*, 229−237.
(56) Feng, Q.; Ferrer, M.; Green, M. L. H.; Mountford, P.; Mtetwa, V. S. B. *J. Chem. Soc., Dalton Trans.* **1992**, 1205−1215.
(57) Abugideiri, F.; Gordon, J. C.; Poli, R.; Owens-Waltermire, B. E.; Rheingold, A. L. *Organometallics* **1993**, *12*, 1575−1582.
(58) Green, M. L. H.; Morise, X. M.; Hamilton, A. H.; Chernega, A. N. *J. Organomet. Chem.* **1995**, *488*, 73−78.
(59) Willey, G. R.; Woodman, T. J.; Drew, M. G. B. *J. Organomet. Chem.* **1996**, *510*, 213−217.
(60) Fettinger, J. C.; Keogh, D. W.; Poli, R. *J. Am. Chem. Soc.* **1996**, *118*, 3617−3625.

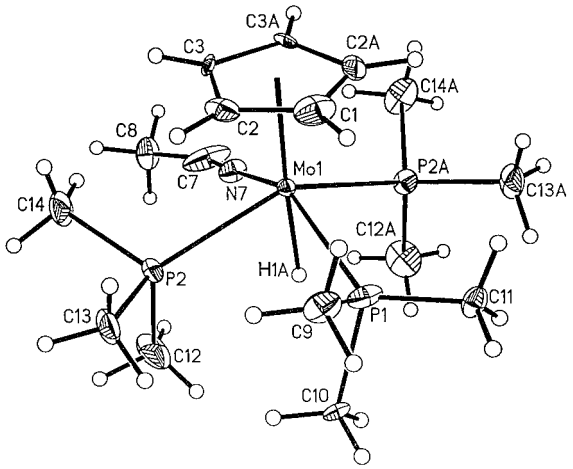

Figure 2. View of the cation for [CpMoH(PMe$_3$)$_3$(MeCN)]$^{2+}$ with the numbering scheme used. Ellipsoids are drawn at the 30% probability level.

trans-influence arguments, the Mo−P(2) bond is significantly longer than the Mo−P(1) bond. No noticeable *trans*-effect, on the other hand, is exerted by the hydride ligand on the Cp ring, since the Mo−CNT distance of 1.97(1) or 1.98(1) Å for the two orientations of the ring in **3** is essentially indentical to the distance of 1.99(1) Å reported for complex [CpMoFCl(dppe)(MeCN)]$^+$, where the ring is located *trans* relative to the weakly *trans*-directing fluoride ligand.[60]

(c) Disproportionation Mechanism. Upon one-electron oxidation of a metal hydride complex [M]−H, the formation of a 1:1 mixture of the protonation product {[M]H$_2$}$^+$ and the solvato complex {[M](S)}$^+$, as in eq 2, is frequently observed. There have been two established mechanisms for this process, both involving the decomposition of the primary oxidation product, the 17-electron {[M]−H}$^{\bullet+}$ complex. These are the deprotonation mechanism[16] and a less commonly observed disproportionation[44,62] mechanism (paths *a* and *b* in Scheme 2, respectively). This disproportionation pathway has previously been proposed for the decomposition of complexes [MH(dppe)$_2$]$^+$ (M = Rh, Ir),[62] [IrH(CO)(PPh$_3$)$_3$]$^+$,[62] [CpReH$_2${P(*p*-XC$_6$H$_4$)$_3$}$_2$]$^+$ (X = H, Me, F, OMe),[53] and [CpRuHL$_2$]$^+$ (L = PPh$_3$ or L$_2$ = Ph$_2$PCH$_2$CH$_2$CH$_2$PPh^2).[44] The deprotonation mechanism involves rate-determining proton transfer to the unoxidized parent hydride complex, while the disproportionation mechanism involves rate-determining electron transfer between two molecules of the primary oxidation product. The disproportionation mechanism also involves a proton transfer, but only after the electron transfer generates a supposedly more acidic {[M](S)H}$^{2+}$ species. For the deprotonation mechanism to occur, the proton transfer from the 17-electron {[M]−H}$^{\bullet+}$ complex to the neutral 18-electron precursor must be very rapid and compete with the oxidation reaction itself. The results of the reactions 1−3 show that the 17-electron complex [**1**]$^+$ is not rapidly deprotonated by **1**, allowing the one-electron oxidation to proceed quantitatively. Then complex [**1**]$^+$ may only decompose by disproportionation since there is no residual **1** left in solution. This proposition is in agreement with kinetic studies, which are presented in the next section. The present system has allowed, *for the first time, the isolation and characterization of the dicationic hydride intermediate of the disproportionation process.* Previously, the existence of this intermediate had only been inferred from electrochemical studies.[44]

The dicationic hydride product is selectively obtained if the oxidation is carried out in the presence of 2 rather than 1 equiv of oxidizing agent. Coordination of the solvent to the 17-electron primary oxidation product to afford a more easily oxidizable 19-electron species probably occurs as shown in Scheme 2.[44] This is indicated by the longer lifetime of the 17-electron species [**1**]$^+$ in the weaker coordinating THF solvent ($t_{1/2}$ = 30 min) relative to MeCN (complete-in less than 7 min). A similar solvent effect has been noticed[44] for the decomposition of [CpRuH(PMe$_3$)$_2$]$^+$ by disproportionation.

The observation of the dication (and indeed its isolation as **3**), even when only 1 equiv of oxidant is used, shows that the final proton-transfer step of the disproportionation mechanism is slow. This has been independently verified by mixing equivalent amounts of the isolated complexes **1** and **3** (eq 4). The steric bulk of the reagents probably hinders the proton transfer. Deprotonation of the dication also occurs slowly upon addition of triethylamine. This reaction affords a spectroscopically pure solution of a single product, corresponding to the complex that forms together with the dihydride cation [CpMoH$_2$(PMe$_3$)$_3$]$^+$ during the decomposition reaction and confirms the assignment of this product to the MeCN adduct [CpMo(PMe$_3$)$_3$(MeCN)]$^+$ (eq 2). Under the reasonable assumption that this reaction follows a second-order rate law, the measured half-life under pseudo-first-order conditions (see Experimental Section) yields an approximate rate constant of 3×10^{-3} s^{-1} M^{-1} for the proton transfer to NEt$_3$. A qualitative comparison indicates that the proton transfer to **1** is slower than to NEt$_3$.

$$[\mathrm{CpMoH(PMe_3)_3(MeCN)}]^{2+} + \mathrm{B} \rightarrow [\mathrm{CpMo(PMe_3)_3(MeCN)}]^{+} + \mathrm{BH}^{+} \quad (4)$$

(B = **1**, NEt$_3$)

(d) Kinetic Studies on the Decomposition of Complex [1]$^+$ in THF. A kinetic handle on the decomposition of [**1**]$^+$ was gained through the time evolution of the EPR spectrum for the reaction carried out in THF (Figure 3, curve a). The data fit well a second-order decay equation (correlation coefficient R^2 = 0.983), while the first-order (exponential) decay gives a much poorer fit (R^2 = 0.929). This is as expected for the disproportionation mechanism (rate = $k_{\mathrm{disprop}}[\mathbf{1}^+]^2$; $k_{\mathrm{disprop}} = 7.5(8) \times 10^{-3}$ s^{-1} M^{-1}). The isolation of **2** when using 2 equiv of oxidant is consistent with this finding and leads us to believe that the kinetic results obtained in THF (rate law and mechanism) may be extrapolated to MeCN, where the decomposition is too fast to be followed by EPR spectrocopy. Complex [CpMo(PMe$_3$)$_3$(S)]$^+$ is unfortunately stable only when S = MeCN, whereas the THF compound leads to further complex decomposition.

The decay of the EPR signal was also studied in the presence of residual neutral starting material **1**, which

(61) Abugideiri, F.; Fettinger, J. C.; Pleune, B.; Poli, R.; Bayse, C. A.; Hall, M. B. *Organometallics* **1997**, *16*, 1179−1185.
(62) Pilloni, G.; Schiavon, G.; Zotti, G.; Zecchin, S. *J. Organomet. Chem.* **1977**, *134*, 305−318.

Downloaded by CARLI CONSORTIUM on June 30, 2009
Published on November 21, 1998 on http://pubs.acs.org | doi: 10.1021/om9805786

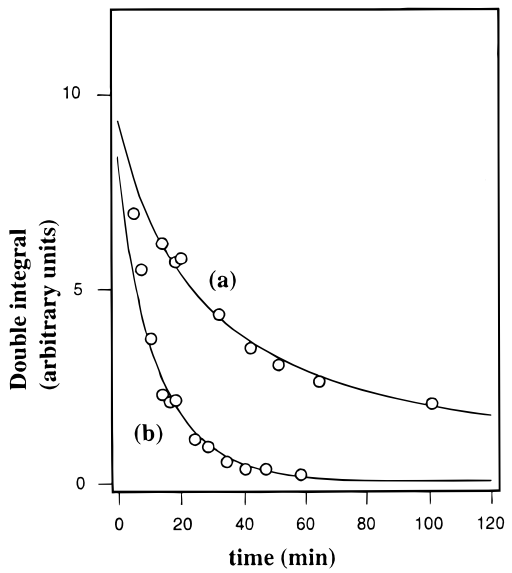

Figure 3. Plot vs time of the EPR signal double integrals for (a) $[\mathbf{1}]^+$ (0.02 M) and (b) $[\mathbf{1}]^+$ (0.02 M) + **1** (0.025 M). The curves are the best fits to the data (see text).

Scheme 2

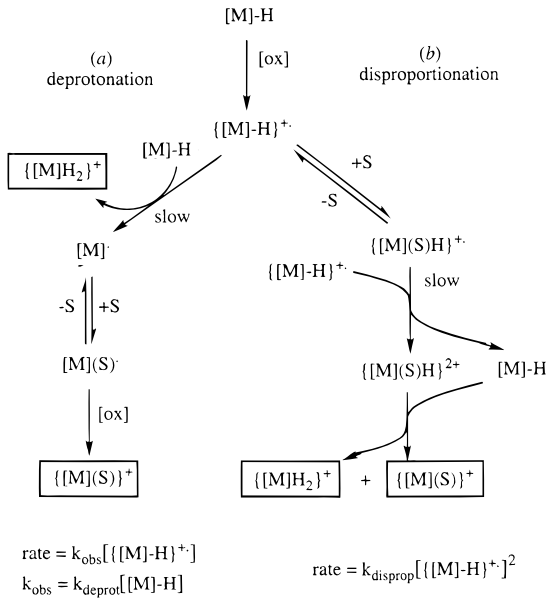

may act as a base according to Scheme 2 (path *a*). A much faster decay was observed under these conditions (see Figure 3, curve b), suggesting that a faster proton-transfer decomposition mechanism is indeed taking place under these conditions. As shown in Scheme 2, the rate law should show a first-order dependence on the radical species and a first-order dependence on the neutral complex for the deprotonation mechanism. In addition, we know that the deprotonated radical complex, $CpMo(PMe_3)_3$, does not accumulate in solution since the EPR monitoring only shows the decay of the signal of $[\mathbf{1}]^+$. Thus, it is likely that $CpMo(PMe_3)_3$ is further oxidized (possibly after coordination of a solvent molecule) by the residual $[\mathbf{1}]^+$ according to eq 5.

$$CpMo(PMe_3)_3 + [\mathbf{1}]^+ + S \rightarrow [CpMo(PMe_3)_3(S)]^+ + \mathbf{1} \quad (5)$$

The comparison of path *a* in Scheme 2 and eq 5 illustrates that compound **1** is consumed by the proton transfer step but is later regenerated by the electron-transfer step. Thus, compound **1** merely acts as a catalyst of the decomposition of $\mathbf{1}^+$ by the deprotonation mechanism. In other words, the concentration of **1** remains constant during the decomposition, and a clean first-order decay is expected. On the other hand, the data give a poor fit for both the first-($R^2 = 0.955$) and the second-order ($R^2 = 0.953$) decay equations. We then reasoned that the decomposition of $[\mathbf{1}]^+$, under these conditions, would be taking place by a combination of the two independent mechanisms. The first-order decay should become prevalent toward the end of the decomposition, when the concentration of $\mathbf{1}^+$ is low, while the decay at the very beginning should follow the disproportionation pathway to a greater extent.[63] The decay should therefore follow the biphasic rate law in eq 6, which provides the integrated rate law shown eq 7 in a straightforward manner. In this equation, $[\mathbf{1}^+]_0$ is the starting concentration of the radical complex, $k_2 = k_{disp}$, and $k_1 = k_{deprot}[\mathbf{1}]$.

$$-\mathrm{d}[\mathbf{1}^+]/\mathrm{d}t = k_1[\mathbf{1}^+] + k_2[\mathbf{1}^+]^2 \quad (6)$$

$$\ln\left(\frac{k_1 + k_2[\mathbf{1}^+]}{[\mathbf{1}^+]}\right) - \ln\left(\frac{k_1 + k_2[\mathbf{1}^+]_0}{[\mathbf{1}^+]_0}\right) = k_1 t \quad (7)$$

Fitting of the data by eq 7 was carried out by imposing k_2 to be identical with the rate constant obtained from the fit of curve a. This yields curve b in Figure 3 for an improved correlation coefficient $R^2 = 0.968$. The value obtained for k_1 is 1.00(7) s^{-1}, which in turns gives $k_{deprot} = k_1/[\mathbf{1}] = 4.4(3) \times 10^{-2}$ s^{-1} M^{-1}. The ratio $k_{deprot}/k_{disp} = 5.8(7)$ means that, when the concentration of **1** is the same as that of $\mathbf{1}^+$, the deprotonation pathway is ca. 5.8 times faster (in the THF solvent) than the disproportionation pathway or, in other words, that $\mathbf{1}^+$ is ca. 5.8 times more likely to transfer a proton to **1** than to oxidize another molecule of $\mathbf{1}^+$ (in equilibrium with $[CpMoH(PMe_3)_3(THF)]^+$) in the THF solvent. In MeCN, the disproportionation pathway should be accelerated as predicted by the better coordinating power of the solvent.[44] The rate of proton transfer from $\mathbf{1}^+$ to **1**, on the other hand, should be essentially solvent independent. If anything, the deprotonation should become slower in MeCN in view of the more favorable equilibrium of formation of the 19-electron solvent adduct, which should in turn have a lower acidity because of the higher metal electron density. In conclusion, the decomposition of $\mathbf{1}^+$ takes place by disproportionation in MeCN, whereas there is a competition between deprotonation and disproportionation in THF, the former being prevalent in the presence of **1**. This appears to be the first hydride system for which a competition between the two decomposition mechanisms has been quantitatively assessed.

The effect of the PMe_3 substitution on the stability of the 17-electron hydride radical species, $[CpMoH(CO)_n(PMe_3)_{3-n}]^+$, toward deprotonation is remarkable. This increased stabilization should probably be attributed to the steric crowding by the bulkier PMe_3 ligand and not to the decreased acidity of the hydride complex. In fact,

(63) Wilkins, R. G. *Kinetics and Mechanism of Reactions of Transition Metal Complexes*, 2nd ed.; VCH: New York, 1991.

Downloaded by CARLI CONSORTIUM on June 30, 2009
Published on November 21, 1998 on http://pubs.acs.org | doi: 10.1021/om9805786

Downloaded by CARLI CONSORTIUM on June 30, 2009
Published on November 21, 1998 on http://pubs.acs.org | doi: 10.1021/om9805786

while the acidity of $[CpMoH(CO)_n(PMe_3)_{3-n}]^+$ decreases as n decreases, the basicity of the proton acceptor $CpMoH(CO)_n(PMe_3)_{3-n}$ correspondingly increases, so that the thermodynamic driving force for the proton transfer should not be greatly affected by the CO/PMe_3 substitution. A similar steric argument has previously been advanced to explain the lack of proton-transfer reactivity for the 17-electron $[Cp^*FeH(dppe)]^+$ complex.[64]

It is also interesting to compare the rates of proton transfer of the 17-electron complex $[\mathbf{1}]^+$ and the 18-electron complex $[CpMoH(PMe_3)_3(MeCN)]^{2+}$ to **1**. The deprotonation of $[\mathbf{1}]^+$ ($k = 5.5 \times 10^{-2}$ s^{-1} M^{-1}) is faster than that of the dicationic hydride ($k < 3 \times 10^{-3}$ s^{-1} M^{-1}), at odds with an expected greater thermodynamic acidity for the dicationic product. We can tentatively rationalize this phenomenon, once again, on steric grounds. The increased steric crowding resulting from the MeCN coordination may render the proton less accessible and the deprotonation kinetically slower.

(e) Protonation of 1. While the addition of H^+ to compound $CpMoH(CO)_2(PMe_3)$ affords an unstable $[CpMo(H_2)(CO)_2(PMe_3)]^+$ complex, which immediately expels H_2,[40] the protonation of the electron richer complex **1** affords the stable dihydride complex $[CpMoH_2(PMe_3)_3]^+$.[38] This protonation reaction was previously investigated in Et_2O/H_2O.[38] We find the same result in MeCN, confirming that the observed complex $[CpMo(PMe_3)_3H_2]^+$ may be obtained in this solvent by proton transfer following the oxidation of **1**. The BF_4 salt (compound **4**) was isolated in high yields by protonation with HBF_4 in toluene. The NMR characterization that we have obtained for this complex completes that previously reported[38] and shows that the compound is a classical dihydride with inequivalent hydride ligands (decoalesced at 238 K in the ^{1}H NMR). A pseudooctahedral structure similar to that described for compound **3** with one pseudoaxial and one pseudoequatorial hydride ligand is suggested by the NMR double-resonance experiments (see supplemental figure). The proposed arrangement is equivalent to that observed by X-ray crystallography for the isoelectronic complex $CpMoH_3(PMe_2Ph)_2$.[61] A similar geometry has also been found through heteronuclear double-resonance experiments and an X-ray diffraction study for the isoelectronic complex $(C_6H_5Me)WH_2(PMe_3)_3^{2+}$.[65] It is rather remarkable that the dihydride cation does not have any tendency to evolve dihydrogen. No change in the NMR spectrum was observed upon standing in CD_3CN for several months or upon heating. The difference in H_2 evolution reactivity between $[CpMoH_2(CO)_n(PMe_3)_{3-n}]^+$ ($n = 1$ and 3) is in line with theoretical studies[66] on the equilibrium between classical and nonclassical polyhydrides for cyclopentadienyl complexes.

Conclusions

We have shown in this contribution that complex **1** undergoes a one-electron oxidation when reacted with Ag^+ or Fc^+, to afford a relatively stable 17-electron hydride product, $[\mathbf{1}]^+$. Hydride complexes with a 17-electron configuration are usually rather unstable. Complex $[\mathbf{1}]^+$ is, to the best of our knowledge, the first such complex for Mo(III) that is sufficiently stable to be characterized spectroscopically. A kinetic study of its decomposition reaction by EPR spectroscopy shows a solvent-assisted disproportionation pathway (faster in MeCN relative to THF). The key intermediate of this pathway, a dicationic hydrido Mo(IV) complex, has been isolated and structurally characterized. The presence of unoxidized **1**, however, catalytically triggers a faster decomposition (in THF) by a deprotonation pathway. It was not possible to establish whether the silver oxidation is direct (outer-sphere) or whether it takes place via the formation of an intermediate Mo−(μ-H)−Ag adduct (inner-sphere mechanism), because no intermediate of this type could be observed. In the next contribution,[35] we shall compare the current findings with those obtained for the oxidation of the related $CpMoH(CO)_2(PMe_3)$ complex.

Acknowledgment. We are grateful to the DOE (Grant DEFG059ER14230) for support of this work.

Supporting Information Available: A figure collecting the ^{1}H NMR, simulated ^{1}H NMR, ^{1}H{selective ^{1}H} NMR, and ^{1}H {selective ^{31}P} NMR spectra in the hydride region for complex $[CpMoH_2(PMe_3)_3]^+$ at 283 K. For the X-ray structure of $[CpMoH(PMe_3)_3(MeCN)][BF_4]_2$·MeCN: tables of crystal data and refinement parameters, fractional coordinates, bond distances and angles, isotropic thermal parameters, and calculated H atom coordinates (10 pages). Ordering information is given on any current masthead page.

OM9805786

(64) Hamon, P.; Toupet, L.; Hamon, J.-R.; Lapinte, C. *Organometallics* **1992**, *11*, 1429−1431.

(65) Green, M. L. H.; Hughes, A. K.; Lincoln, P.; Martin-Polo, J. J.; Mountford, P.; Sella, A.; Wong, L.-L.; Bandy, J. A.; Banks, T. W.; Prout, K.; Watkin, D. J. *J. Chem. Soc., Dalton Trans.* **1992**, 2063−2069.

(66) Lin, Z.; Hall, M. B. *Organometallics* **1992**, *11*, 3801−3804.